JOURNAL OF KUFA−PHYSICS
journal.uokufa.edu.iq/index.php/jkp/index | ISSN: 2077−5830

Tunneling magnetoresistance calculation for double quantum dot connected in parallel shape to ferromagnetic Leads

*** Laith. N. R** **T. A. Salman**

Physics Department, College of Science, University of Basra, Basra, Iraq .

*Corresponding Author E-mail: laith.n.ramdhan@gmail.com

ARTICLE INF

Article history:
Received: 06 MAR, 2023
Revised: 09 APR, 2023
Accepted: 27 APR, 2023
Available Online: 28 JUN, 2023

Keywords:

quantum dots
ferromagnetic leads
Green's function
Conductance
tunneling magnetoresistance

ABSTRACT

In this paper, a theoretical model for electron transport through symmetric system consisting of two baths interferometer with one single-level quantum dot in each of its arms was considered. In this model, the dots are attached to ferromagnetic leads with parallel and antiparallel magnetic configurations. Green's function technique in this model was used. Our focus is on the Transport characteristics of conductance (G) and tunnel magnetoresistance (TMR). A special attention to the influence of an applied magnetics flux on the characteristics of conductance and tunneling magnetoresistance was paid. Concerning the study of the conductance, it was found that the effect of bonding (antibonding) states is most obvious in quantum dots at various values of the magnetic field. The change in spin-polarization value was seen to affect the increase and decrease in the conductance value. We noticed a difference in calculation of TMR in the bonding and the antibonding states, where the results show Strong dissonance in bonding state and strong attraction in antibonding state.

DOI: http://doi.org/10.31257/2018/JKP/2023/v15.i01.11428

حساب مقاومة النفق المغناطيسية لنقطتين كميتين مربوطتين بشكل متوازي ومتصلتين بقطبين فيرومغناطيسيين

ليث نزار رمضان **طالب عبد النبي سلمان**

قسم الفيزياء – كلية العلوم – جامعة البصرة-البصرة-العراق

الكلمات المفتاحية:

النقاط الكمية
الأقطاب الفيرومغناطيسية
دالة كرين
التوصيلية
مقاومة النفق المغناطيسية

الـــخُـــلاصــــة

في هذه الورقة، تم تقديم أنموذج نظري لنقل الإلكترون خلال نظام متماثل متضمن مسارين لمقياس تداخل يحتوي كل مسار فيه على نقطة كمية ذات مستوي طاقة واحد والنظام متصل بقطبين فيرومغناطيسيين يتشكل البرم فيهما بشكل موازي وغير موازي نسبة الى أحد القطبين. ولقد تم استخدام تقنية دالة كرين لحل معادلة الحركة للنظام. اهتمامنا تركز على مميزات التوصيلية وحساب مقاومة النفق المغناطيسية تحت تأثير مجال مغناطيسي خارجي. في دراستنا للتوصيلية، توصلنا الى ان تأثير حالة الارتباط (عدم الارتباط) هي الاكثر شيوعاً

في النقاط الكمية لقيم مختلفة من المجال المغناطيسي. أن التغير في قيمة البرم المستقطب يؤثر علـى زيـادة ونقصـان مقـدار التوصـيلية. نلاحـظ وجـود اخـتلاف فـي حسـاب مقاومـة النفـق المغناطيسية فـي حالـة الارتبـاط وعـدم الارتبـاط، حيـث أظهـرت النتـائج تنـافر قـوي فـي حالـة الارتباط وتجاذب قوي في حالة عدم الارتباط

1. INTRODUCTION

In the last few years, Quantum dots (QDs) structures have attracted much attention due to ability to use in theoretical studies and industrial applications [1,2], in which electrons are confined in three-dimensional system of the nanometer scale [3]. One of the most important features of quantum dots is the possibility of adjusting their energy gap with complete accuracy by changing the size of QD where the size of QD is inversely proportional to its energy gap [4]. Also, it has sharp density of state which is a good characteristic of electronic transitions and optical properties in detectors [5]. In addition, quantum dots have many future applications like Medical applications, quantum computing, QD Laser, QD LED, white light sources, single electron transistor, QD solar cells..etc. [6–8]. Recently the transport properties through tunnel-coupled double QDs system in series or parallel configuration connected to external leads has widely been spread in scientific research because it has similar behavior of molecules and called in most time “artificial molecules” [9,10]. It’s considered as an ideal system to study the fundamental multi-body interactions in quantum transport between single electron and spins [11]. Also, it has richer physical phenomena to study, especially a parallel-coupled dots has one of most important effects is the Fano effect [12]. When external leads made from Ferromagnetic materials, the transport properties of hole system will be strongly dependent on the relative orientation of electrodes magnetizations [13,14], leading us to tunneling magnetoresistance (TMR) effect, spin accumulation and exchange field, etc. [15,16]. Regarding the TMR, it can describe the change in resistance of a system when the magnetic orientation of two electrodes varies from parallel (same spin orientation in both electrodes) to antiparallel (different spin orientation in both electrodes) configuration [17]. The TMR effect is very important to develop magnetic sensors and magnetic storge devices such as magneto resistive random-access memory (MRAM) [18]. In the past years, spin-polarized tunneling experiments results between a superconductor and a ferromagnet, lead the way to present field-dependent tunneling between Ferromagnetic films. Julliere put his model for FM–I–FM tunneling [19,20], where Julliere model assumed that spin is conserved in tunneling and tunnel current depends on the density of states of the two electrodes [11]. Experimentally observation Prove that the electrical resistance of the insulator barrier depends on the relative alignment of the magnetic moments of the electrodes [21], we

can Denoting the conductance in parallel alignment by (G_P) and antiparallel alignment by (G_{AP}), TMR will define in terms of resistance as:

$$TMR = \frac{G_P - G_{AP}}{G_{AP}} \tag{1}$$

In this paper, we shall discuss a mathematical model to calculate the transmission coefficient and the conductance for the system of two parallel quantum dots and we show how we calculate the (TMR) by using the equation of motion for retarded Green function. In this study, we should use ferromagnetic leads to include spin-polarization effect in our calculation for TMR.

2. THE MATHEMATICAL MODEL

In this work, two single Level-dots connected in parallel shape with two ferromagnetic leads, as illustrated in Fig. 1.

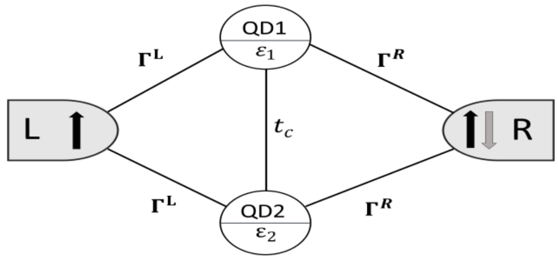

Figure 1: A Double Quantum dot connected in parallel shape to the ferromagnetic Leads.

The parallel connection of the Double dots can provide two Path to electrons transfer from the left Lead (L) to the right Lead (R). The Transition rate between the dots and Leads are ($\boldsymbol{\Gamma^L}$) and (Γ^R), also the dots are connected to each other by tunneling rate (t_c). Therefore, the total Hamiltonian is expressed as follows:

$$\hat{H} = \hat{H}_{Leads} + \hat{H}_{Dots} + \hat{H}_{tunneling} \qquad (2)$$

Where we can write each term of the Eq. (2) as in below:

$$\hat{H}_{Leads} = \sum_{k\alpha\sigma} \varepsilon_{k\alpha} C^{\dagger}_{k\alpha\sigma} C_{k\alpha\sigma}$$
(3)

Where K is the wave vector of electrons inside the electrodes and α indicates the left and right Leads (L and R), σ describes the direction of electrons spin (σ=↑↓). ($\varepsilon_{k\alpha}$) represents the energy levels of the electrodes, ($C^{\dagger}_{k\alpha\sigma}$) *and* $C_{k\alpha\sigma}$ are the (creation) annihilation catabolism and growth influences of conduction electrons respectively at the α electrode.

$$\hat{H}_{dots} = \sum_i \varepsilon_i d^{\dagger}_{i\sigma} d_{i\sigma}$$
$$-t_c \sum_{\sigma} (d^{\dagger}_{i\sigma} d_{2\sigma} + d^{\dagger}_{2\sigma} d_{i\sigma})$$
(4)

where i represents the first and second numeral dot, ε_i is the energy levels within the quantum dot, ($d^{\dagger}_{i\sigma}$) *and* $d_{i\sigma}$ are growth and the catabolism effect of the electrons at the quantum dot, respectively.

$$\hat{H}_{\text{Interaction}} \sum_{k\alpha i\sigma} t_{\alpha i\sigma} \left(C^{\dagger}_{k\alpha\sigma} d_{i\sigma} + d^{\dagger}_{i\sigma} C_{k\alpha\sigma} \right) \quad (5)$$

where $t_{k\alpha i\sigma}$ is the interaction energy between the quantum dot and the Leads. The Line width (Γ) is related to $t_{k\alpha i\sigma}$ as:

$$\Gamma = \sum_k t_{\alpha\sigma} t^{*}_{\alpha\sigma} (2\pi\delta(\varepsilon - \varepsilon_{k\alpha})$$
(6)

Here, we consider the wide band approximation to energy band in the Leads, so (Γ) doesn't depend on energy and we take it as a constant. we can write $\Gamma = \Gamma^L + \Gamma^R$ Where:

$$\Gamma^L = \frac{\Gamma}{2} \begin{bmatrix} 1 & e^{i\frac{\phi}{2}} \\ e^{-i\frac{\phi}{2}} & 1 \end{bmatrix} ، \Gamma^R = \frac{\Gamma}{2} \begin{bmatrix} 1 & e^{-i\frac{\phi}{2}} \\ e^{i\frac{\phi}{2}} & 1 \end{bmatrix} \quad (7)$$

where Φ is the magnetic phase factor. We can define the Line width (Γ) in terms of an electron spin-polarization parameter P_α for the two leads, with $\Gamma_L = \Gamma(1 \pm P_L)$, $\Gamma_R = \Gamma(1 \pm P_R)$, the quantity $\Gamma = (\Gamma^{L/R}_{\text{ii}\uparrow} + \Gamma^{L/R}_{\text{ii}\downarrow})/2 = 1$ is set to be the energy unit. We consider the parallel $P_L = P_R = P$ and the antiparallel $P_L = -P_R = P$ configurations of the two leads. To calculate the conductance, G, of the System we must find first the transmission factor, $T(\omega)$, where the conductance related to $T(\omega)$ by:

$$G = \frac{2e^2}{h} T(\omega)$$
(8)

To calculate $T(\omega)$, we must use the equation of motion method of the Green function of the dots. The retarded Green function of the quantum dot is given by [22]:

$$G^R_{ij}(t, t') = -i\theta(t) < \{ d_{i\sigma}(t), d^{\dagger}_{j\sigma}(t') \} >$$
(9)

Here, we use t'=0

$\theta(t)$ is the unit's steep function, and $d_{i\sigma}(t)$, $d^{\dagger}_{j\sigma}(t')$ are defined in equation (4).

$$T(\omega) = trace(G^A(\omega)\Gamma^R G^R(\omega)\Gamma^L) \qquad (10)$$

$G(\omega)$ is Fourier transformation of $G(t)$

by the use of the relation for the operator $C_{k\alpha\sigma}(t)$ which is given by:

$$C_{k\alpha\sigma}(t) = e^{iHt} C_{k\alpha\sigma} e^{-iHt}$$
(11)

Where H is defined in equation (2), and $C_{k\alpha\sigma}$ doesn't depend on time, we can get.

$$\frac{d}{dt} C_{k\alpha\sigma}(t) = iHe^{iHt} C_{k\alpha\sigma} e^{-iHt} + e^{iHt} C_{k\alpha\sigma}(-iH) e^{-iHt}$$
(12)

Differentiate equation (9) and using equation (12) we can obtain:

$$i\frac{d}{dt} G_{ij}^{R}(t) = \delta(t).\delta_{ij} + i\theta(t)$$

$$.< \left\{ i e^{iHt}[C_{k\alpha\sigma}, H] e^{-iHt}, d_{j\sigma}^{\dagger}(\mathrm{t}) \right\} > \quad (13)$$

We must find $[C_{k\alpha\sigma}, H]$ by using equation (2), so we obtain two equations, one for quantum dots and other for Leads [23]:

$$i\frac{d}{dt} G_{ij}^{R}(t) = \delta(t).\delta_{ij} + \varepsilon_i G_{ij}^{R}(t) + \sum_{k\alpha\sigma} t_{\alpha i\sigma}^{*} G_{k\alpha\sigma}^{R}(t) \quad (14)$$

And other one is:

$$i\frac{d}{dt} G_{k\alpha\sigma}^{R}(t) = \varepsilon_{k\alpha} G_{k\alpha\sigma}^{R}(t) + \sum_i t_{\alpha i\sigma} G_{ij}^{R}(t)$$
(15)

Using Fourier transformation for equation (14) and (15) with some simplification, we find:

$$G_{11} = \frac{\left(\omega - \varepsilon_2 + i\frac{\Gamma}{2}\right)}{\frac{\Gamma^2}{4}cos^2\frac{\varphi}{2} + (\omega - \varepsilon_1 + i\frac{\Gamma}{2})(\omega - \varepsilon_2 + i\frac{\Gamma}{2})}$$

$$G_{12} = \frac{-icos\frac{\varphi}{2}}{\frac{\Gamma^2}{4}cos^2\frac{\varphi}{2} + \left(\omega - \varepsilon_1 + i\frac{\Gamma}{2}\right)\left(\omega - \varepsilon_2 + i\frac{\Gamma}{2}\right)}$$

$$G_{22} = \frac{\left(\omega - \varepsilon_1 + i\frac{\Gamma}{2}\right)}{\frac{\Gamma^2}{4}cos^2\frac{\varphi}{2} + (\omega - \varepsilon_1 + i\frac{\Gamma}{2})(\omega - \varepsilon_2 + i\frac{\Gamma}{2})}$$

$$G_{21} = \frac{-icos\frac{\varphi}{2}}{\frac{\Gamma^2}{4}cos^2\frac{\varphi}{2} + \left(\omega - \varepsilon_1 + i\frac{\Gamma}{2}\right)\left(\omega - \varepsilon_2 + i\frac{\Gamma}{2}\right)} \quad (16)$$

And $G^R(\omega) = \begin{pmatrix} G_{11} & G_{12} \\ G_{21} & G_{22} \end{pmatrix}$ (17)

Using equation (16) and (17), we get:

$$G^R(\omega) = \frac{1}{\frac{\Gamma^2}{4}cos^2\frac{\varphi}{2} + \left(\omega - \varepsilon_1 + i\frac{\Gamma}{2}\right)\left(\omega - \varepsilon_2 + i\frac{\Gamma}{2}\right)} * \begin{pmatrix} \omega - \varepsilon_2 + i\frac{\Gamma}{2} & -i\frac{\Gamma}{2}cos \\ -i\frac{\Gamma}{2}cos\ \frac{\varphi}{2} & \omega - \varepsilon_1 + i \end{pmatrix}$$
(18)

Equation (18) represents retarded Green function which we find by Solving the equation of motion, after we are finding retarded Green function (G^R), now, it's easier to find $T(\omega)$ which is defined in equation (10). The first diagonal term in the result of the multiplication $T(\omega) = \begin{pmatrix} T_{11} & T_{12} \\ T_{21} & T_{22} \end{pmatrix}$ is:

$$T_{11} = (\omega - \varepsilon_2)^2 + \frac{\Gamma^2}{4} - i\Gamma\cos\frac{\varphi}{2}e^{-i\frac{\varphi}{2}}\left(\omega - \varepsilon_2 - i\frac{\Gamma}{2}\right) + i\frac{\Gamma}{2}\cos\frac{\varphi}{2}e^{i\frac{\varphi}{2}}\left(\omega - E_2 + i\frac{\Gamma}{2}\right) + \frac{\Gamma^2}{2}\cos^2\frac{\varphi}{2} + \left(\omega - \varepsilon_2 - i\frac{\Gamma}{2}\right)\left(\omega - E_1 + i\frac{\Gamma}{2}\right)e^{-i\varphi} + i\frac{\Gamma}{2}cos\frac{\varphi}{2}\left(\omega - E_1 + i\frac{\Gamma}{2}\right)e^{-i\frac{\varphi}{2}} \quad (19)$$

And the last element form is:

$$T_{22} = (\omega - \varepsilon_1)^2 + \frac{\Gamma^2}{4} + \frac{\Gamma^2}{2}\cos^2\frac{\varphi}{2} + i\frac{\Gamma}{2}\cos\frac{\varphi}{2}\left(\omega - \varepsilon_1 + i\frac{\Gamma}{2}\right)e^{i\frac{\varphi}{2}} + \left(\omega - \varepsilon_2 - i\frac{\Gamma}{2}\right)\left(\omega - \varepsilon_1 + i\frac{\Gamma}{2}\right)e^{i\varphi} - i\Gamma\cos\frac{\varphi}{2}e^{i\frac{\varphi}{2}}\left(\omega - \varepsilon_2 - i\frac{\Gamma}{2}\right) + i\frac{\Gamma}{2}\cos\frac{\varphi}{2}e^{-i\frac{\varphi}{2}}\left(\omega - \varepsilon_1 + i\frac{\Gamma}{2}\right) \quad (20)$$

So, the transmission coefficients, $T(\omega)$ is:

$$T(\omega) = T_{11} + T_{22}$$

$$T(\omega) = \frac{\Gamma^2\left(\cos^2\frac{\varphi}{2}(\omega - \bar{E})^2 + \left(\frac{\Delta E}{2}\right)^2\sin^2\frac{\varphi}{2}\right)}{\left[(\omega - \bar{E})^2 - \left(\frac{\Delta E}{2}\right)^2 - \frac{\Gamma^2}{4}\sin^2\frac{\varphi}{2}\right]^2 + [\Gamma(\omega - \bar{E})]^2} \quad (21)$$

where $\bar{E} = (\varepsilon_1 + \varepsilon_2)/2$, $\Delta E = \varepsilon_2 - \varepsilon_1$

We can include tunneling Energy, t_c, between the two dots in $T(\omega)$ as:

$$T(\omega) = \frac{\Gamma^2\left(\cos^2\frac{\varphi}{2}(\omega-\bar{E})^2+\left(\frac{\Delta E-2t_c}{2}\right)^2\sin^2\frac{\varphi}{2}\right)}{\left[(\omega-\bar{E})^2-\left(\frac{\Delta E-2t_c}{2}\right)^2-\frac{\Gamma^2}{4}\sin^2\frac{\varphi}{2}\right]^2+[\Gamma(\omega-\bar{E})]^2} \quad (22)$$

Using equation (8) and equation (20) to reach the conductance, then we can calculate the tunneling magnetoresistance (TMR) by following equation (1) form, which is dependent on relative orientation of Leads magnetization.

3. RESULT AND DISCUSSION

3.1 Calculation of linear conductance, (G)

In this subsection, we discussed the linear conductance as function of Femi level for different parameters, where we used equation (4) to calculate the linear conductance for parallel(antiparallel) magnetization configuration of leads.

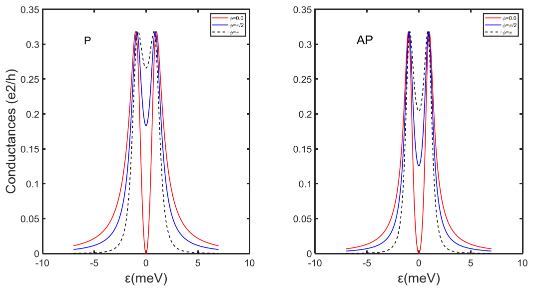

Figure 2: Linear conductance as a function of Fermi Level, when $t_c = 0.5\, meV$, $\boldsymbol{\varepsilon_1} = \boldsymbol{\varepsilon_2} = 0.5\, meV$, $P = 0.3$. (left) parallel lead-configuration; (Right) antiparallel lead-configuration.

Figure 2 demonstrates the evolution of conductance by setting tunneling Energy, $t_c = 0.5\, meV$, the linear conductance for parallel(antiparallel) configuration shows two relatively broad peaks related to anti-bonding-like states, with deep minimum in between, where the conductance turns to zero at $\phi = 0$ due to destructive interference of electron waves transmitted from dot (1) and dot (2), worth noting that more increasing in lines broadening for Parallel configuration than antiparallel configuration due to the effect of spin-polarization (P), also we will notice the effect of spin-polarization very clearly in next figures.

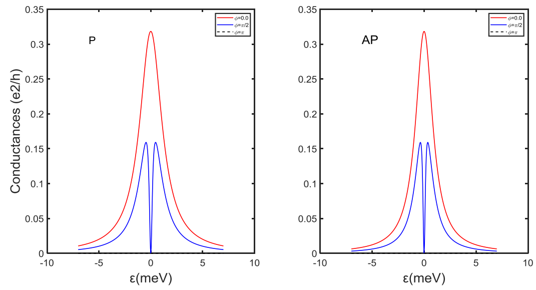

Figure 3: Linear conductance as a function of Fermi Level, when $t_c = -0.5\, meV$, $\boldsymbol{\varepsilon_1} = \boldsymbol{\varepsilon_2} = 0.5\, meV$, $P = 0.3$. (left) parallel lead-configuration; (Right) antiparallel lead-configuration.

Figure 3 demonstrates the evolution of conductance by setting tunneling Energy, $t_c = -0.5\, me$, the spectrum shape shows one broad Peak at $\phi = 0$ due to strictive interference of electron waves transmitted from dot (1) and dot (2) at same time, for $\phi = \pi/2$ we can see two relatively broad peaks, with sharp deep minimum in between , where the conductance turns to zero due to destructive interference of electron waves transmitted from quantum dots (dot 1, dot 2). For $\phi = \pi$ the conductance equal to zero because of the change in phase factor of electron waves transmitted from dot (1) and dot (2). Now to understand the effect of spin-polarization on conductance, we will use same scenario and parameters in previous figures (Fig.2-Fig.3), but with change spin-polarization (P) value at that time, see (Fig.4-Fig.7).

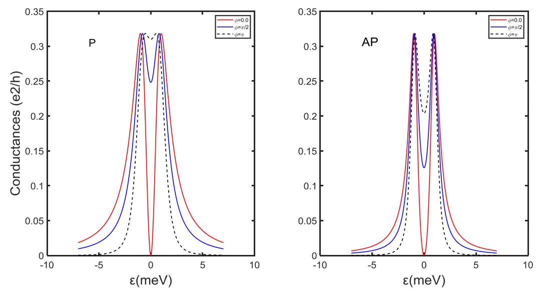

Figure 4: Linear conductance as a function of Fermi Level, when $t_c = 0.5\, meV$, $\boldsymbol{\varepsilon_1} = \boldsymbol{\varepsilon_2} = 0.5\, meV$, $P = 0.7$. (left) parallel lead-configuration; (Right) antiparallel lead-configuration.

From Fig.4 and by compare with Fig. 2, we can see for (parallel configuration), the increment of polarization gave more broadening of the spectrum lines and change dips positions for $\phi = \pi/2$ and $\phi = \pi$, for $\phi = 0$ the dip became more Sharpe if we compare with previous value of spin-polarization in Fig.2, for (antiparallel configuration) the polarization not effect in the conductance behavior. Same behavior observed by increasing Spin-polarization to 0.9, see Fig.6.

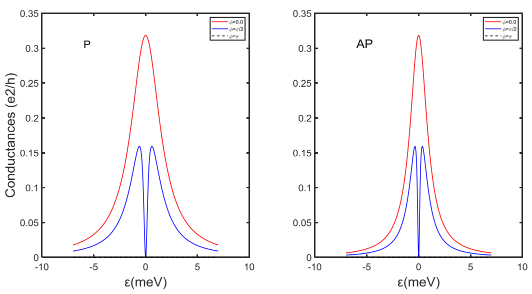

Figure 5: Linear conductance as a function of Fermi Level, when $t_c = -0.5\, meV$, $\boldsymbol{\varepsilon_1} = \boldsymbol{\varepsilon_2} = 0.5\, meV$, $P = 0.7$. (left) parallel lead-configuration; (Right) antiparallel lead-configuration.

From Fig.5 and by comparing with Fig.3, we can see for (parallel configuration), the spin polarization effect on the broadening of Spectrum with no change in peaks positions, for (antiparallel configuration), the increasement of Polarization never change conductance behavior. We obtained the same characteristics of conductance by increasing spin-polarization to 0.9, see Fig.7.

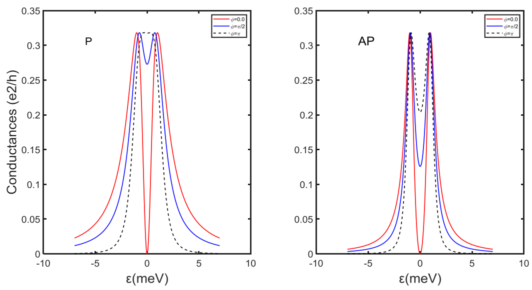

Figure 6: Linear conductance as a function of Fermi Level, when $t_c = 0.5\, meV$, $\boldsymbol{\varepsilon_1} = \boldsymbol{\varepsilon_2} = 0.5\, meV$, $P = 0.9$. (left) parallel lead-configuration; (Right) antiparallel lead-configuration.

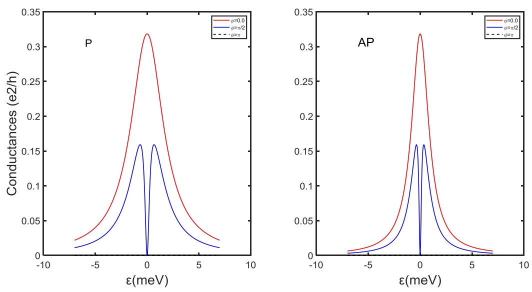

Figure 7: Linear conductance as a function of Fermi Level, when $t_c = -0.5\, meV$, $\boldsymbol{\varepsilon_1} = \boldsymbol{\varepsilon_2} = 0.5\, meV$, $P = 0.9$. (left) parallel lead-configuration; (Right) antiparallel lead-configuration.

We will examine the effect of increasement for tunneling energy and dot Levels at this time, so we will repeat our calculation for the conductance with various value of polarization. In Fig.8, we can notice the increment of tunneling energy and dot Levels, make the peaks almost matching for all values of Φ, also change dips position and give more increasing in spectrum broadening for both P(AP) configurations. In Fig.9, it can be seen that the increment of tunneling energy and dots did not have an effect on conductance behavior related to $\bar{E}$ and $\Delta\varepsilon$.

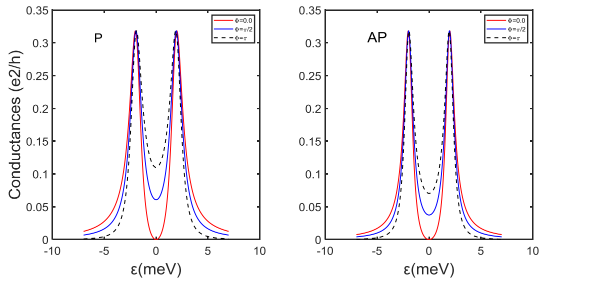

Figure 8: Linear conductance as a function of Fermi Level, when $\mathrm{t_c} = 1.0\, meV$, $\boldsymbol{\varepsilon_1} = \boldsymbol{\varepsilon_2} = 1.0\, meV$, $P = 0.3$. (left) parallel lead-configuration; (Right) antiparallel lead-configuration.

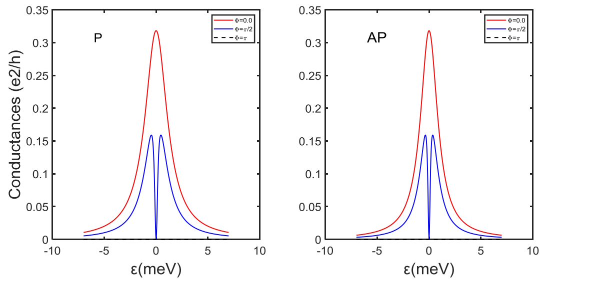

Figure 9: Linear conductance as a function of Fermi Level, when $\mathrm{t_c} = -1.0\, meV$, $\boldsymbol{\varepsilon_1} = \boldsymbol{\varepsilon_2} = 1.0\, meV$, $P = 0.3$. (left) parallel lead-configuration; (Right) antiparallel lead-configuration.

3.2 Calculation of tunneling magnetoresistance, (TMR)

In this subsection, we discussed the tunneling magnetoresistance (TMR) as function of Fermi level for different Parameters. The TMR now follows equation (1) form. In our study for TMR, we show the characteristics of magnetic flux phase factor (ϕ) with different Values of tunneling Energy ($\mathrm{t_c}$), then we will Repeat our calculation for TMR but with increase spin-polarization at that time, to see the effect of (P) on TMR. In Fig.10, we can see two Symmetrical dips with one peak at center when ($\varepsilon = 0$) for all Values of ϕ and spectrum interference has been observed. In Fig.11 by change tunneling Energy to -0.5 meV, we can see negative peaks in TMR appears for $\Phi = \pi/2$ and $\Phi = \pi$, for $\Phi = 0$ the TMR drop to zero when ($\varepsilon = 0$) due to destructive interference of electron waves transmitted from dot (1) and dot (2).

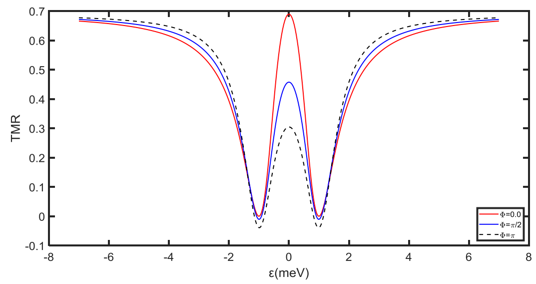

Figure 10: TMR as a function of Fermi Level, when $\mathrm{t_c} = 0.5\, meV$, $\boldsymbol{\varepsilon_1} = \boldsymbol{\varepsilon_2} = 0.5\, meV$, $P = 0.3$.

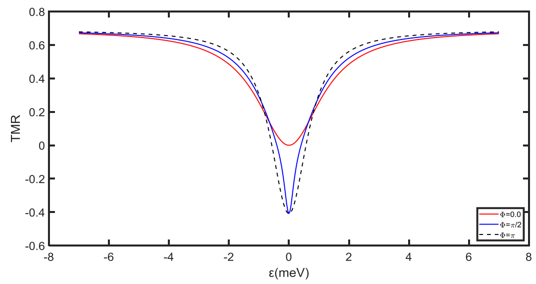

Figure 11: TMR as a function of Fermi Level, when $\mathrm{t_c} = -0.5\, meV$, $\boldsymbol{\varepsilon_1} = \boldsymbol{\varepsilon_2} = 0.5\, meV$, $P = 0.3$.

Now, we will repeat our calculation for TMR with increase polarization Value, to see the effect of (P) on TMR behavior. From Fig.12 and with comparison with Fig.10, we can see that spin-polarization gives high increase in Spectrum broadening for all values of Φ, also change peaks positions.

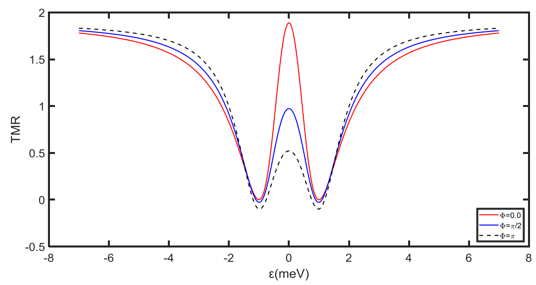

Figure 12: TMR as a function of Fermi Level, when $\mathrm{t_c} = 0.5\, meV$, $\boldsymbol{\varepsilon_1} = \boldsymbol{\varepsilon_2} = 0.5\, meV$, $P = 0.7$.

4. CONCLUSIONS

In this work, we have analyzed the influence of external magnetic flux on the conductance, G, and tunneling magnetoresistance, TMR. For (antibonding) State, the conductance shows two relatively broad peaks, with deep minimum in between for both magnetic configuration and for all values of Φ, also by increase spin-polarization value we observed for (parallel configuration), more broadening of the spectrum lines and change in positions of dips for $\phi = \pi/2$ and $\phi = \pi$, for $\phi = 0$ where the dip became more Sharpe, for (antiparallel configuration), the polarization did not affect in the conductance behavior. For (bonding) state, the conductance shows one broad peak at $\phi = 0$ and two relatively broad peaks, with sharp deep minimum in between at $\phi = \pi/2$, for $\phi = \pi$ the conductance equal to zero, also by change spin-polarization we found in (parallel configuration), the spin polarization effect on the broadening of Spectrum with no change in peaks positions, for (antiparallel configuration), the increasement of Polarization never change conductance behavior. The effect of the magnetic field is produced by deflecting the spinning of the electron passing through the system. As a result of this deviation, the shape of the spectrum changes according to the change in the phase angle resulting from the effect of the field. For TMR, we noticed that negative Value of TMR appear for bonding State when ($\varepsilon = 0$) due to Strong dissonance, while TMR show positive value for antibonding state because of strong attraction, also we consider the effect of spin-polarization on this case, where spin-polarization give more increasing in Spectrum broadening for all values of Φ and changed peaks positions.

5. REFERENCES

[1] T. A. S. M. T. Dhahir, "Electron Transport Through Two Branch Interferometer with Rashba Spin Orbit Interaction." Basrah Journal of Science, vol. 39, no. 3, pp. 398–413, 2021.

[2] A. M. Bagher, "Quantum Dots Applications," Sensors & Transducers, vol. 198. IFSA, pp. 37–43, 2016.

[3] M. A. Najdi, H. A. Jassem, and J. M. Al-Mukh, "Electron tunneling through serially coupled double quantum dots: The coulomb blockade," in IOP Conference Series: Materials Science and Engineering, vol. 454, no. 1, 2018

[4] A. A. and S. D. Alireza Valizadeh, Haleh Mikaeili, Mohammad Samiei, Samad Mussa Farkhani, Nosratalah Zarghami, Mohammad kouhi, "Quantum dots: synthesis, bioapplications, and toxicity Alireza." Nanoscale Res. Lett., 2012.

[5] V. G. M. V Martynenko, V A Kuznetsova, A O Orlova, P A Kanaev, A. V. B. and A Loudon, V Zaharov, P Parfenov, Yu K Gun'ko, and A. V Fedorov, "Chlorin e6–ZnSe/ZnS quantum dots based system as reagent for photodynamic therapy." Nanotechnology, 2015.

[6] R. E. Bailey, A. M. Smith, and S. Nie, "Quantum dots in biology and medicine," Physica E: Low-Dimensional Systems and Nanostructures, vol. 25, no. 1. pp. 1–12, 2004.

[7] A. Datta, A. Shaji, and C. M. Caves, "Quantum discord and the power of one qubit," Physical Review Letters, vol. 100, no. 5, 2008.

[8] S. Sriphan, S. Kiravittaya, S. Thainoi, and S. Panyakaew, "Effects of Temperature on I-V Characteristics of InAs/GaAs Quantum-Dot Solar Cells," Advanced Materials Research, vol. 1103. pp. 129–135, 2015.

[9] D. Sztenkiel and R. Świrkowicz, "Electron transport through parallel double quantum dots with interdot correlations," in Physica Status Solidi (B) Basic Research, vol. 244, no. 7, pp. 2543–2548, 2007.

[10] Abbas. A. Hashim and T. A. Selman, "Tunneling Current Calculation in Double Quantum Dots." Basrah Journal of Science (A) , vol. 36, no. 1, pp. 16–28, 2018.

[11] I. Weymann, "Effects of different geometries on the conductance, shot noise, and tunnel magnetoresistance of double quantum dots," Phys. Rev. B - Condens. Matter Mater. Phys., vol. 78, no. 4, 2008.

[12] G. H. Ding, C. K. Kim, and K. Nahm, "Fano resonance in electron transport through parallel double quantum dots in the Kondo regime," Phys. Rev. B - Condens. Matter Mater. Phys., vol. 71, no. 20, 2005.

[13] I. Weymann, "Tunnel magnetoresistance and linear conductance of double quantum dots strongly coupled to ferromagnetic leads," J. Appl. Phys., vol. 117, no. 17, 2015.

[14] G. Michałek and B. R. Bułka, "Tunnel magnetoresistance in quantum dots in the presence of singlet and triplet states," J. Phys. Condens. Matter, vol. 23, no. 17, 2011.

[15] N. T. Xue, H. Q. Xie, H. B. Xue, and J. Q. Liang, "Effect of spin exchange interaction on shot noise and tunnel magnetoresistance in double quantum dots," Phys. E Low-Dimensional Syst. Nanostructures, vol. 59, pp. 163–168, 2014.

[16] C. Z. Ye, W. T. Lu, and C. T. Xu, "Spin accumulation in the parallel-coupled double quantum dots with Rashba spin-orbit interaction connected with ferromagnetic and superconducting electrodes," Mod. Phys. Lett. B, vol. 29, no. 25, 2015.

[17] F. Chi, H. Zeng, and X. Yuan, "Flux-dependent tunnel magnetoresistance in parallel-coupled double quantum dots," Superlattices Microstruct., vol. 46, no. 3, pp. 523–532, 2009.

[18] S. Yuasa, T. Nagahama, A. Fukushima, Y. Suzuki, and K. Ando, "Giant room-temperature magnetoresistance in single-crystal Fe/MgO/Fe magnetic tunnel junctions," Nature Materials, vol. 3, no. 12. pp. 868–871, 2004.

[19] J. S. Moodera and L. R. Kinder, "Ferromagnetic-insulator-ferromagnetic tunneling: Spin-dependent tunneling and large magnetoresistance in trilayer junctions (invited)," in Journal of Applied Physics, vol. 79, no. 8 PART 2A, pp. 4724–4729, 1996.

[20] J. MATHON, "Theory of Tunneling Magnetoresistance," EBSCO Publ., vol. 76, no. 4–5, pp. 491–500, 2003.

[21] W. H. Butler, X. G. Zhang, S. Vutukuri, M. Chshievand, and T. G. Schulthess, "Theory of tunneling magnetoresistance for epitaxial systems," in IEEE Transactions on Magnetics, vol. 41, no. 10, pp. 2645–2648, 2005.

[22] H. J. Xue, T. Q. Lü, H. C. Zhang, H. T. Yin, L. Cui, and Z. L. He, "Thermopower in parallel double quantum dots with Rashba spin-orbit interaction," Chinese Phys. B, vol. 20, no. 2, 2011.

[23] M. T. Dhahir, "Theoretical Study of the Thermopower of Two Parallel Quantum Dots in the presence of Rashba Spin - Orbit," University of Basra, 2022.